PERGAMON

International Journal of Heat and Mass Transfer 43 (2000) 4405–4418

International Journal of HEAT and MASS TRANSFER

www.elsevier.com/locate/ijhmt

Flow and impingement cooling heat transfer along triangular rib-roughened walls

C. Gau*, I.C. Lee

Institute of Aeronautics and Astronautics, National Cheng Kung University, Tainan 70101, Taiwan, ROC

Received 28 September 1999; received in revised form 10 February 2000

Abstract

Experiments are performed to study slot air jet impingement cooling flow and the heat transfer along triangular rib-roughened walls. Both flow visualization and local heat transfer measurements along the ribbed wall are made. The effect of different rib protrusions (heights) on the impinging flow and heat transfer along the wall is studied, which is achieved by using different sizes of nozzles. Two different ribbed walls with different rib pitches are selected which have a rib pitch-to-height ratio of 2 and 4, respectively. The widely opened cavity between neighboring ribs make more intense transport of momentum between the wall jet and cavity flow so that recirculation cell in the cavity is hardly observed. This leads to a higher heat transfer around the cavity wall than in the case with rectangular ribs. However, in the region of laminar wall jet, a number of air bubbles enclosing the cavities are formed which prevent penetration of the wall jet into the cavities. This leads to a significant reduction in the heat transfer. The geometric shape of the triangular ribs is more effective in rebounding the wall jet away from the wall than in the case with rectangular ribs. The rebound of the jet away from the wall causes a significant reduction in the heat transfer. A comparison and correlations of the stagnating point Nusselt number under different conditions are presented and discussed. During the experiments, the Reynolds number varies from 2500 to 11,000, the slot width-to-rib height ratio from 1.17 to 6.67, and nozzle-to-plate spacing from 2 to 16.

1. Introduction

Impingement cooling heat transfer has been studied extensively in the past due to its wide application in cooling the walls of high temperature thermal systems. The air-jet impinging normally on the wall can remove a large amount of heat over a relatively small surface area. It has been frequently used in cooling the hottest section of a combustion chamber or a turbine blade. A good review article on the study of impingement cooling flow and heat transfer is available [1,2]. The impingement cooling for jet from a single rectangular or round nozzle or an array of nozzles over a heated surface has been well studied [3–6]. Correlations of stagnation point, local and average Nusselt number in terms of relevant nondimensional parameters have been obtained.

Studies in the past are mostly on a flat and smooth surface [1–10] with relatively few over a curved surface [11,12]. In a practical consideration, however, in order to enhance the heat transfer on the surface, one of the alternatives is to use a roughened wall. The roughened wall has been fre-

* Corresponding author. Tel.: +886-6-2757-575; fax: +886-6-2389-940.

E-mail address: gauc@mail.ncku.edu.tw (C. Gau).

0017-9310/00/$ - see front matter
PII: S0017-9310(00)00064-8

Nomenclature

A	area of a heat strip
b	slot width
c_p	specific heat
e	rib height
h	convective heat transfer coefficient
I	current
k	thermal conductivity
Nu	Nusselt number, hb/k
p	rib pitch
Pr	Prandtl number, $c_p\mu/k$
q	heat flux
Re	Reynolds number, $U_j b/\nu$
T	temperature
Tu	turbulence intensity
U	streamwise velocity
V	voltage
x	lateral distance from the stagnation point
z	slot-to-plate spacing or the axial distance of the jet from the nozzle exit
μ	viscosity
ν	kinematic viscosity

Subscripts

a	refers to ambient air
aw	refers to adiabatic wall
j	refers to jet flow at slot exit
o	refers to stagnation point
w	refers to wall

quently used inside or outside of a tube to enhance the heat transfer [13]. For impingement cooling over a roughened wall, only few works are found [14]. The roughened wall was made with parallel rectangular ribs attached to a heated wall. It was found [14] that in some situations the heat transfer along the roughened wall is indeed significantly enhanced. However, when the slot-width-to-rib-height is small, most of the flow stream of the wall jet can be trapped into the cavity between neighboring ribs which can significantly reduce the heat transfer. In addition, the spacing between neighboring rectangular ribs close to the stagnation point may be an ideal place to induce an air bubble enclosing the cavity, which can prevent penetration of impinging jet into the cavity and recirculation inside. This can significantly reduce the heat transfer on and around the stagnation point. Therefore, in order to rectify the drawbacks mentioned above, triangular ribs are used in the current work. This will provide a widely opened spacing between neighboring ribs where recirculation flow may not be so easily trapped in and stay there; at the same time air bubbles enclosing the cavity may not be so easily formed as in the case when the rectangular ribs are used. Therefore, a higher heat transfer is expected with the triangular rib-roughened wall.

The objective of the present experiments is to study the impingement cooling flow structure and heat transfer enhancement over the triangular rib-roughened walls. The heating condition considered is a heated flat wall with the placement of small triangular ribs. The flat plate is heated electrically by passing a current through a 0.015 mm thin stainless steel foil so that a constant heat flux boundary condition along the wall can be achieved. The local Nusselt number distributions along the ribbed wall are measured. The flow structure is visualized with smoke that is generated by vaporising oil coated over a heated resistance wire. During the experiments, a total of four nondimensional parameters, i.e. the Reynolds number, the slot width-to-rib height ratio, the nozzle-to-plate spacing and the rib pitch-to-height ratio, that affect the local Nusselt number distribution are selected to vary. For convenience, the variation of the slot width-to-rib height ratio is achieved by using different sizes of nozzle. Two different cases of the impingement cooling process are considered. Case A considers the situation when the cooling jet is directed towards the rib, while case B considers when it is directed towards the center line of the cavity. A better understanding of the process is provided.

2. Experimental apparatus and procedures

The impinging air jet issued from the nozzle is supplied with a high pressure blower system which can furnish a maximum air flow of 10 m^3/min. To ensure air quality, a settling chamber with a honeycomb and different sizes of meshes is made and used to reduce the turbulence intensity and maintain a uniform air flow at the exit. The nozzle is made convergent and curved smoothly which allows rapid acceleration of fluid without the occurrence of flow separation and generation of turbulence. Therefore, uniform velocity profile associated with a relatively low turbulence intensity across the nozzle width at the exit is obtained. The streamwise turbulence intensity at the nozzle exit is measured with a hot wire anemometer and is found to be less than 0.7% for Reynolds number ranging from 2500 to 11,000. The jet velocity is measured with

a Pitot tube. A total of four different sizes of rectangular nozzles are made, which are 0.35, 0.6, 1.2 and 2 cm in wide, respectively. To ensure that the second dimension of the nozzle slot does not affect the slot-jet flow, all the nozzles are made long in the direction perpendicular to the nozzle axis which is 15 cm in length.

A schematic of the apparatus is shown in Fig. 1. The rib-roughened wall is 20 cm wide and 50 cm long. It consists of a 1 cm thick Plexiglas, a 0.015 mm thin stainless steel foil which is adhered on the top of the Plexiglas, and a number of 3 mm high and 3 mm wide eqvilateral triangular rib elements which are mounted and glued in parallel on the foil surface. The ribbed wall can be heated by passing electric current through the thin foil. The layer of glue between the ribs and the foil is made thin enough so that the thermal resistance is negligible while the electric resistance is large to prevent the electric current circulating through the ribs. All the ribs are equally spaced. Two different ribbed walls having different rib pitches, i.e. 6 and 12 mm, are made, which have a rib pitch-to-height ratio p/e of 2 and 4, respectively. Since the steel foil is so thin and the Plexiglas wall has a very low thermal conductivity, the heat conduction along the wall is negligibly small. To reduce heat loss to the ambient, the heated surface is well insulated on the back. To account for the additional radiation heat loss directly from the steel foil, the total heat loss to the ambient is estimated at less than 3%.

To measure the temperature distribution along the heated wall, a total of 58 thermocouples are inserted individually into equally spaced small holes drilled in the wall in order that the thermocouple junction can be attached to the heated steel foil. Since all the thermocouples are placed under the ribs (not on top of them), this allows us to study the enhancement of the momentum and heat transfer due to the addition of the rib elements on a heated flat plate. The pitch between two adjacent thermocouples is 3 mm. Therefore, there is one thermocouple located at the position where each rib stands. For a ribbed wall having $p/e = 2$, there is only one equally spaced thermocouple in each cavity, while for the one having $p/e = 4$, there are three thermocouples in each cavity. One additional thermocouple is used to measure the jet temperature at the slot exit. All the temperature signals are acquired with a data logger and sent into a PC for data processing and plotting. Before the experiments, all the thermocouples are calibrated in a constant temperature bath to ensure the measurement accuracy of $\pm 0.1^{\circ}C$.

To ensure that the stainless steel foil is heated uniformly, the entire foil is cut into a number of long strips. Each strip is heated individually with an equal amount of dc power. With the desired voltage V and current I passing through the thin strip, the heat flux along the surface can be calculated and is equal to VI/A, where A is the area of the strip. The local heat transfer coefficient can be determined with the following equation:

$$h = q/(T_w - T_a) \tag{1}$$

When the jet velocity is greater than 20 m/s, the viscous heating effect along the wall becomes noticeable. At this time, Eq. (1) needs to be modified. This is done by replacing T_a in Eq. (1) by T_{aw}. The adiabatic wall

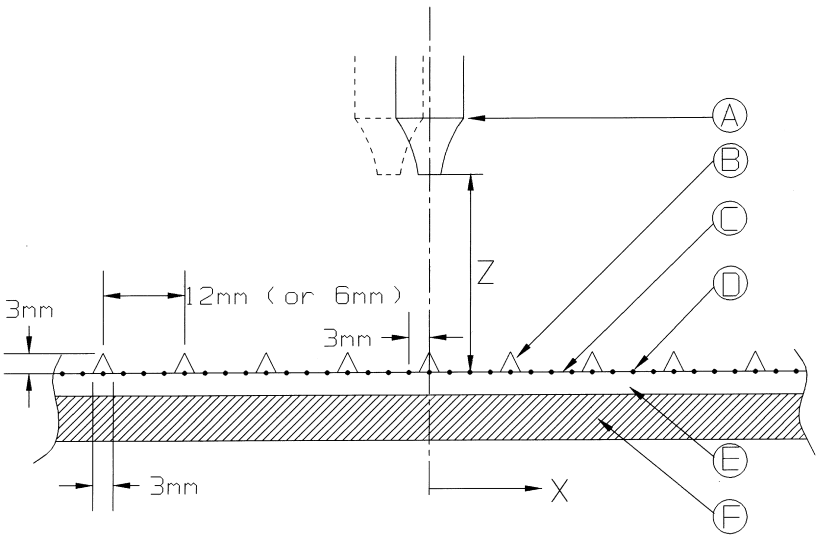

Fig. 1. Schematic of apparatus: (A) rectangular nozzle, (B) triangular rib, (C) stainless steel foil, (D) thermocouples, (E) Plexiglas plate and (F) foamed rubber.

temperature along the surface is measured when the foil heater is turned off. The uncertainty in the experimental data is determined according to the procedure proposed by Kline and McClintock [16]. The maximum uncertainty in local Nusselt number is 5.6%, in the Reynolds number it is 6.2% and the turbulence intensity it is 3.25%.

3. Results and discussion

3.1. Flow visualization

In general, the impinging flow structure observed along the ribbed wall is significantly different from that along a flat plate. Since the triangular shape of ribs can form cavities more widely open than does the rectangular shape of ribs, the impinging jet in the present case is expected to penetrate much more easily into the cavity and recirculate inside. The widely open cavity allows intense momentum transport between the recirculation flow and the wall jet. This makes the recirculation cell hardly seen in the cavity, as shown in Figs. 2–4. For cavity between rectangular ribs, recirculation cell can be clearly observed [14] which persists for a long time. Therefore, a higher momentum transport leads to a higher heat transfer in the current cavity than in the cavity formed by rectangular ribs.

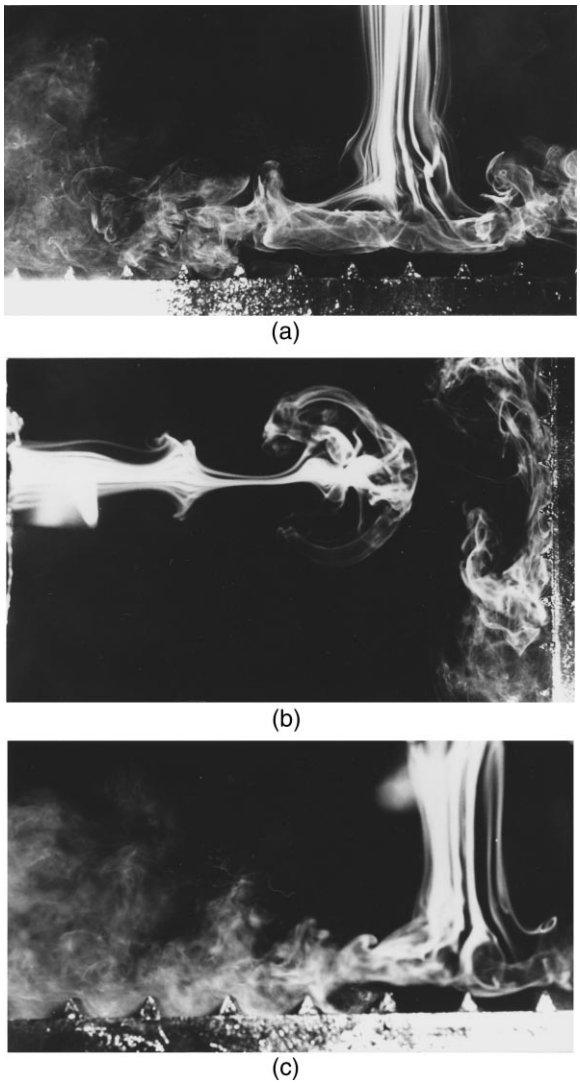

Fig. 2. Wall jet structure along the ribbed wall for $p/e = 4$, $Re = 2500$ and (a) $b/e = 6.67$, $z/b = 4$ (b) $b/e = 6.67$, $z/b = 8$ and (c) $b/e = 4$, $z/b = 4$.

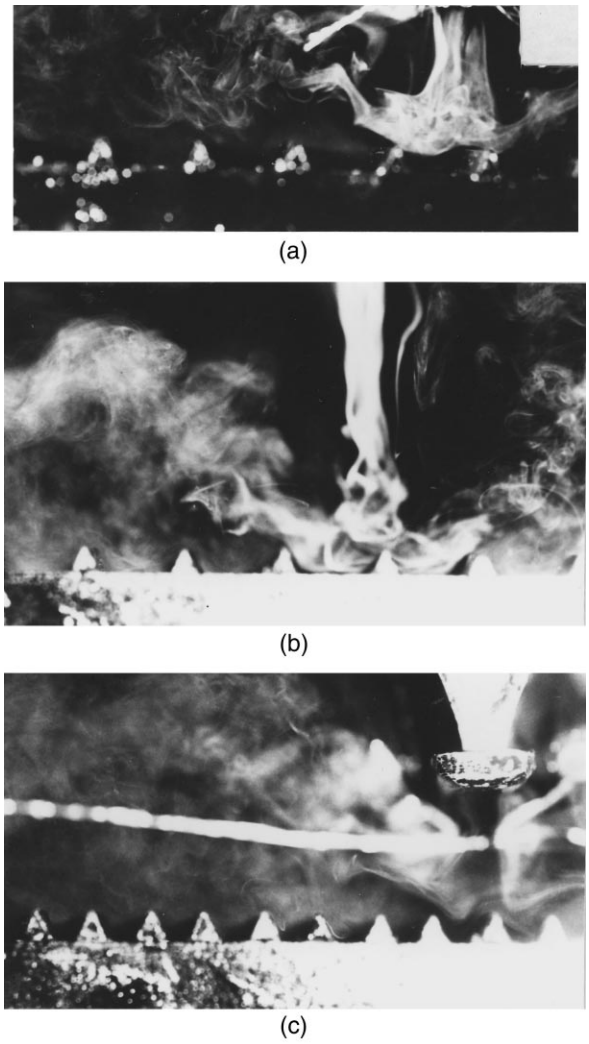

Fig. 3. Wall jet structure along the ribbed wall for $Re = 2500$ and (a) $p/e = 4$, $b/e = 2$, $z/b = 4$ (b) $p/e = 4$, $b/e = 2$, $z/b = 8$ and (c) $p/e = 2$, $b/e = 1.17$, $z/b = 4$.

For $b/e = 6.67$, $p/e = 4$, $z/b = 4$ and $Re = 2500$, a similar air bubble enclosing the cavity as in the case of rectangular cavity, can be observed, as shown in Fig. 2a. This will make the jet turn horizontally and move along the top edge of the ribs when the jet approaches the wall. It appears that close to the stagnation point, the pressure inside the cavity is still significantly higher than outside, and formation of an air bubble enclosing the cavity occurs which prevents the air jet from penetrating into the cavity. The formation of an air bubble also occurs in several cavities downstream along the wall until the wall jet becomes turbulent which can penetrate into the cavity. One can expect that the formation of air bubble along the wall may reduce the heat transfer, while penetration and recirculation of air jet into the cavity can significantly enhance the heat transfer. The latter Nusselt number measurements (Fig. 5a) indicate that significant enhancement of heat transfer occurs when the transition of a laminar wall jet into a turbulent one occurs (i.e. close to $x/b = 4$). This fact confirms the previous expectation.

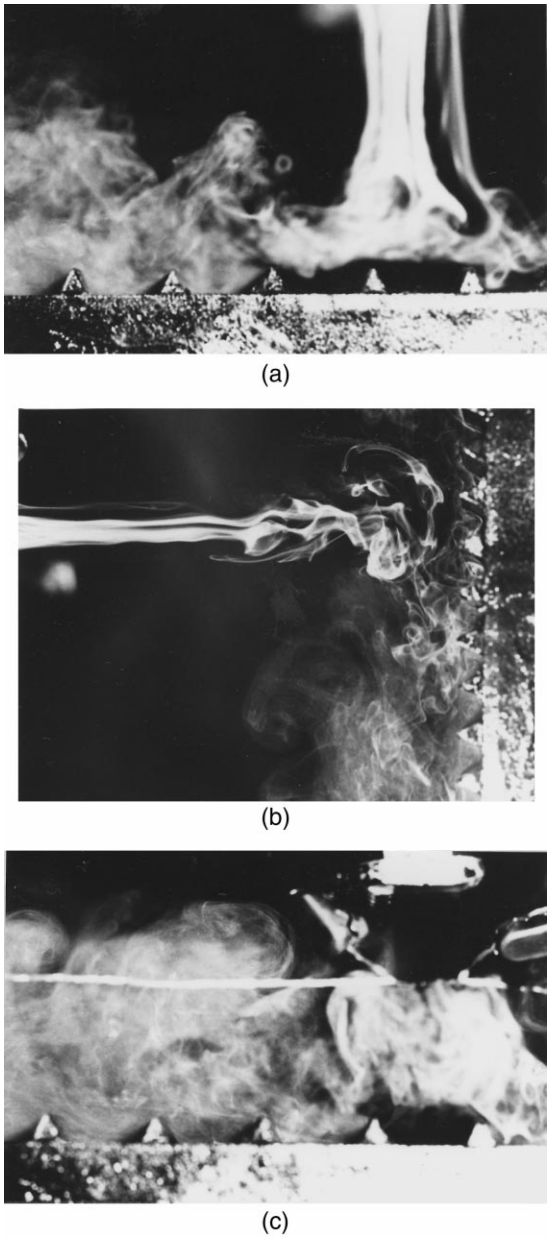

Fig. 4. Wall jet structure along the ribbed wall for case B, $Re = 2500$ and (a) $p/e = 4$, $b/e = 4$, $z/b = 4$ (b) $p/e = 2$, $b/e = 2$, $z/b = 12$ (c) $p/e = 4$, $b/e = 2$, $z/b = 4$.

When the nozzle-to-plate spacing is large, i.e. $z/b \geq 8$, the jet before arriving at the wall becomes wide and fully turbulent. At this stage, the jet can readily penetrate into the cavity and recirculate inside, as shown in Fig. 2b with $z/b = 8$.

As the slot width reduces, the number of air bubbles enclosing the cavities close to the stagnation point is reduced, as shown in Fig. 2c for $b/e = 4$, $p/e = 4$ and $z/b = 4$. This is due to an earlier transition to a turbulent wall jet for an impinging jet issued from a narrower slot. The earlier transition to a turbulent wall jet can also be inferred from the local Nusselt number measurements for impingement cooling along a flat plate [14,15]. Since the transition point is close to $x/b = 4$ for different jets issued from either a wider or a narrower slot, one can expect an earlier transition to a turbulent wall jet when the impinging jet is issued from a narrower slot.

When $b/e \leq 2$, i.e. when the slot becomes narrow, although only one air bubble enclosing the cavity at the stagnation point is still formed, as shown in Fig. 3a for $z/b = 4$, the jet impinging on the wall can rebound and move away from the wall, due to the protrusion of the ribs, and a vacuum can be created in the downstream region. In addition, the vacuum created downstream can suck the air flow and make the jet to move backward and reattach to the wall again. However, the reattached flow is relatively weak. One can expect that the rebound of the wall jet can reduce the heat transfer while the reattachment of jet can increase the heat transfer. For $z/b = 8$, the impinging jet before arriving at the wall has become turbulent, which will penetrate into the air bubble enclosing the cavity and rebound again from the wall due to the protrusion of ribs. However, the rebounded jet can be quickly sucked backwards by the vacuum created downstream and reattached to the wall again. For $z/b = 12$, the impinging jet before arriving at the wall becomes so wide and turbulent that the flow structure can not be clearly observed. One is not sure if the rebound of the impinging jet still occurs. For rectangular cavity, the rebound of the impinging jet occurs only in the extreme con-

dition of $b/e = 1.17$, $z/b = 4$ and $p/e = 4$ [14]. The rebound of the impinging jet was not found at either a greater b/e or z/b. One can be sure, therefore, that the rebound of the jet is related to the geometric shape of the ribs. It appears that the triangular shape of the rib favours rebound of the jet.

For a smaller p/e, the air bubble enclosing the cavity between neighboring ribs close to the stagnation point can still be formed [15]. However, the number of air bubbles formed for smaller p/e is greater than in the case for larger p/e. Since the location for the transition of a laminar wall jet to a turbulent one does not change, i.e. close to $x/b = 4$, the wall jet can be maintained laminar within $x/b \leq 4$ with a greater number of ribs when the pitch of the rib elements is smaller. When b/e reduces, the number of air bubble reduces accordingly as described in the previous case. For $b/e \leq 2$ and $p/e = 2$, the impinging jet on the wall can rebound slightly from the wall but quickly gets sucked backward and reattached to the wall again, as shown in Fig. 3c. The wall jet in the downstream is just like the one when the rebound of wall jet does not occur. The local heat transfer is expected to reduce in the downstream close to the location of rebound, but increases further downstream. The rebound of the wall jet in a smaller pitch ratio ($p/e = 3$) was not found in the cavity formed by the rectangular ribs [14]. This difference is attributed again to the triangular ribs which is favourable to the occurrence of jet rebound.

When the jet is directed towards the center line of the cavity, the flow structure is shown in Fig. 4a–c. When the jet is laminar before arriving at the wall, a similar kind of air bubble enclosing the cavity is observed, as shown in Fig. 4a. Penetration of the wall jet flow into the air bubble and recirculation inside the cavity is not observed until the wall jet becomes turbulent. When the nozzle-to-plate spacing z/b is large and the impinging jet before arriving at the wall becomes turbulent, it can penetrate into the air bubble enclosing the cavity and recirculate inside, as shown in Fig. 4b. The flow structure of the impinging jet for case B is very similar to that of case A when b/e is greater than 2. When $b/e = 2$, the air bubble enclosing the cavity at the stagnation point can still be observed, but no rebound of the wall jet away from the wall is found, as shown in Fig. 4c. For the extreme case when $b/e = 1.17$, the rebound of the jet does occur for $x/b = 4$ [4], but not for $z/b = 8$ when the jet before arriving the wall becomes turbulent and its mixing with the surrounding flow becomes intense. For ribs of rectangular shape, no rebound of the jet away from the wall was found for the case B with $b/e = 1.17$. It appears that the rebound of the jet flow strongly depends on the geometric shape and arrangement of the ribs and the size of the slot width. The protrusion of the ribs and its shape must be in the right position to guide the jet to rebound away from the wall.

3.2. Heat transfer

For impingement cooling over a flat plate, the current data have been validated by comparing with the results of others [3,12] and the agreement was found to be very good. The local Nusselt number has a maxi-

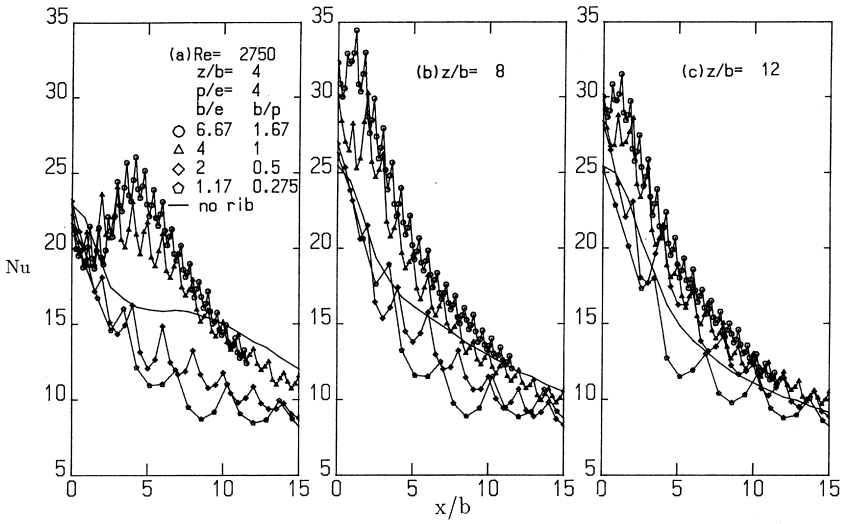

Fig. 5. The Nusselt number distributions at different slot width-to-rib height ratios for the case of $p/e = 4$, $Re = 2750$ and (a) $z/b = 4.0$, (b) $z/b = 8.0$ and (c) $z/b = 12$.

mum at the stagnation point, which decreases monotonically towards downstream. A minimum in the heat transfer for $z/b = 4$ occurs at approximately $x/b = 4$, when a transition from a laminar wall jet into a turbulent one is initiated. The Nusselt number on and around the stagnation point is found to increase with increasing slot width. In the downstream region, however, the local Nusselt numbers for different slot widths approach approximately the same value. However, when comparison was made with the results in reference [14], it was found that the data in reference [14] are 15% higher near the stagnation point region and are 3% higher at the end of the plate than the current data. By checking the raw data of reference [14], this discrepancy is attributed to an erroneous measurement of T_a made in reference [14]. By proper calibration for measurement of T_a, the data in reference [14] are in good agreement with the current data. This comparison further confirms the data measured in the current work.

3.2.1. Effect of slot width-to-rib height ratio on the local Nusselt number

For ribbed walls, the Nusselt number distribution becomes zigzag shaped, as shown in Figs. 5–8. The spikes in the distribution represent the Nusselt number at the locations where the triangular ribs stand, while the lower data points (either three or one) between neighboring spikes representing the ones at the locations of cavities. It appears that the rib protrusion along the wall can significantly increase the heat transfer due to its increase in the surface area and promotion of turbulence. Even the Nusselt number in the cavities of the ribbed wall in most of the region is higher than in the case along the flat plate, as shown in Fig. 5 for $b/e \leq 4$. However, for $z/b = 4$, the enhancement of heat transfer in the region near the stagnation point is not so significant due to occurrence of air bubble enclosing the cavity between neighboring ribs which prevents the cooling of the impinging jet. In most of the following cases, the heat transfer in the region near the stagnation point along the ribbed wall is even lower than along the flat plate due to the occurrence of the air bubbles. However, as the wall jet becomes turbulent, it can penetrate readily into the air bubble, recirculate inside and significantly enhance the heat transfer, as shown in Fig. 5a. However, the protrusion of the rib has an opposite effect of reducing the momentum of the wall jet and effectively reducing heat transfer. As the wall jet moves far downstream, the momentum of the wall jet can be reduced significantly so that heat transfer along the ribbed wall can be much reduced and is lower than in the case of flat plate, as shown in Fig. 5a and b. In general, the Nusselt number decreases with decreasing the slot width (or b/e). This is attributed to the rib protrusion which becomes relatively large and effective in reducing the wall jet momentum and results in reduction in the heat transfer as the wall jet issued from a narrower slot (smaller b/e) becomes relatively thin. For $b/e \leq 2$, the Nusselt number along the ribbed wall is significantly lower than in the case along the flat plate. However, this is attributed to the rebound of wall jet by the protrusion of the ribs, as described previously in the flow

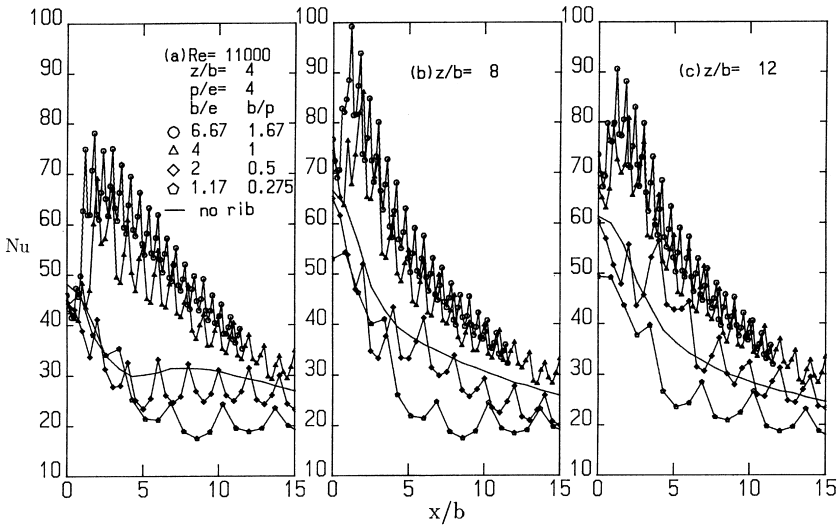

Fig. 6. The Nusselt number distributions at different slot width-to-rib height ratios for the case of $p/e = 4$, $Re = 11{,}000$ and (a) $z/b = 4.0$, (b) $z/b = 8.0$ and (c) $z/b = 12$.

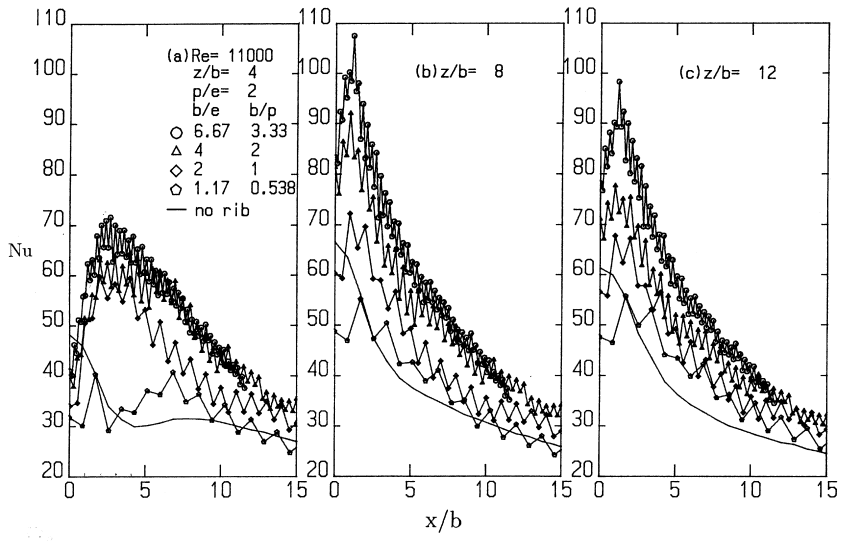

Fig. 7. The Nusselt number distributions at different slot width-to-rib height ratios for the case of $p/e = 2$, $Re = 11{,}000$ and (a) $z/b = 4.0$, (b) $z/b = 8.0$ and (c) $z/b = 12$.

visualization experiment, However, in the downstream the reattachment of the jet is so weak that no significant enhancement in the heat transfer is found.

For the case when $z/b \geq 8$, the impinging jet has become wide and turbulent before arriving at the wall, it can readily penetrate into the cavity between neighboring ribs and recirculate inside. A significant enhancement in the heat transfer is found, as shown in Fig. 5b and c. However, for $z/b = 12$, the impinging jet before arriving at the wall has become so wide and the wall jet flow along the wall has become so thick that the protrusion of the ribs could not effectively reduce its momentum. Therefore, the Nusselt number in the downstream for the ribbed wall with $b/e \geq 4$ is still higher than in the case of the flat plate. When $b/e \leq 2$ and $z/b = 8$, the rebound of wall jet is not so severe as in the case for $z/b = 4$ and the reduction in the heat transfer is not so severe. For $b/e \leq 2$ and

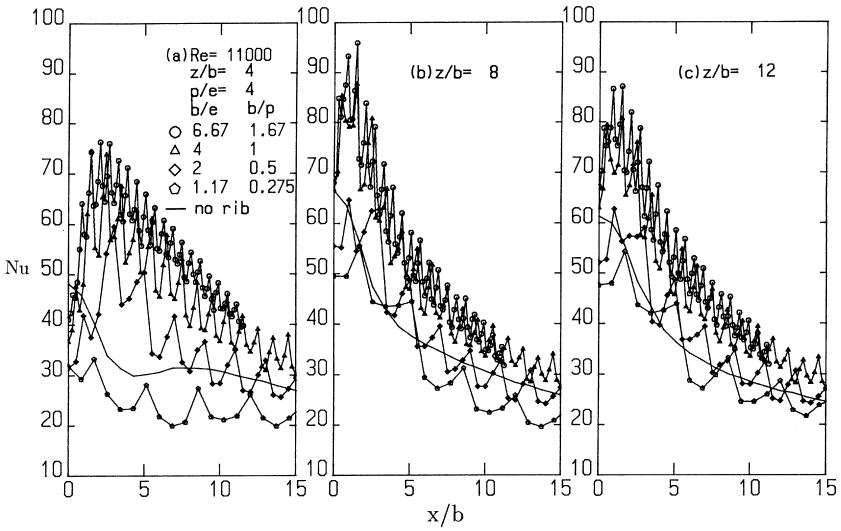

Fig. 8. The Nusselt number distributions at different slot width-to rib height ratios for the case B and $p/e = 4$, $Re = 11{,}000$ and (a) $z/b = 4.0$, (b) $z/b = 8.0$ and (c) $z/b = 12$.

$z/b = 12$, rebound of the impinging jet is not found. However, a significant reduction in the heat transfer is still found. This is the case when the slot-width-to-rib height ratio is small, the wall jet layer is relatively thin as compared with the rib height, the momentum of the wall jet is significantly reduced by the ribs and leads to a significant reduction in the local Nusselt number.

As the Reynolds number increases, similar enhancement in the heat transfer is found, as shown in Fig. 6 for Re = 11,000, except that the local spike in the Nusselt number is much higher. This fact indicates that jet impingement over ribbed wall at higher Reynolds number becomes more effective in enhancing the heat transfer. However, as one compares the local spikes in the Nusselt number between the case along the rectangular ribbed wall and the case along the triangular ribbed wall, the local spikes in the current work is much smaller. The smaller spike in the Nusselt number is mainly attributed to the smaller surface area of the triangular shape of the rib which can dissipate the heat less effectively.

Since the wall jet momentum becomes much higher at higher Reynolds number, the protrusion of the rib becomes ineffective in reducing the wall jet momentum, as in the case of lower Reynolds number heat transfer in the downstream for $b/e \geq 4$ is still higher than the results of the flat plate. Despite this fact, it appears that a higher Reynolds number leads to a shift of the maximum heat transfer towards the stagnation point as one compares Fig. 5a with Fig. 6a. This shift in maximum heat transfer suggests that at higher Reynolds number, the wall jet can penetrate into the cavity at an earlier stage. Similar shift in maximum heat transfer also occurs in rectangular ribbed wall. However, the amount of the shift is much less in the rectangular ribbed wall. It appears that the triangular ribbed wall has a wider cavity that can allow the wall jet readily to penetrate inside at an earlier stage and leads to a larger shift.

The Nusselt number in the region around the stagnation point for $b/e \leq 2$ with $z/b = 8$ and 12 is significantly reduced and is even lower than the results of flat plate, as shown in Fig. 6b and c. This significant reduction in the Nusselt number suggests the occurrence of the air bubbles in the cavities around the stagnation point at higher Reynolds number which prevents penetration of the impinging jet even when it has become turbulent before arriving at the wall. Similar reduction in the stagnation point Nusselt number was also found on the rectangular ribbed wall at this higher Reynolds number and is attributed to the formation of air bubbles which prevents the wall jet cooling effect.

As the pitch of the ribs decreases, the cavity between neighboring ribs becomes narrower. This will make the wall jet difficult to penetrate into the cavity until at later times when the wall jet has become fully turbulent. Therefore, one can see a clear shift of the maximum heat transfer away from the stagnation point as one compares Fig. 7a with Fig. 6a. In addition, the spike in the Nusselt number for $p/e = 2$ is much smaller than for $p/e = 4$. This further suggests that penetration of wall jet into cavity and recirculation inside occurs less likely for $p/e = 2$. For $b/e \leq 2$, the significantly lower heat transfer at the stagnation point at $z/b = 8$ and 12 suggests that formation of air bubble in the cavity which prevents penetration of wall jet and reduces the heat transfer still occurs even when the impinging jet before arriving at the wall has become turbulent. The formation of air bubble enclosing the cavity around the stagnation point still occurs when the Reynolds number is very low, i.e. Re = 2750, and penetration of wall jet into cavity becomes easier. This is attributed again to the smaller opening of the cavity (for $p/e = 2$) which makes it difficult for wall jet to penetrate inside.

When the impinging jet is directed towards the center line of the cavity, the Nusselt number distribution is very similar to the case when the impinging jet is directed towards the rib, as shown in Fig. 8, except in the region around the stagnation point where the Nusselt number is significantly lower. This is apparently due to the formation of air bubble enclosing the cavity around the stagnation point that prevents the air jet from impinging on the wall. It appears that formation of air bubble still occurs even when the wall jet becomes turbulent before arriving at the wall. These findings are very similar to the case along rectangular ribbed wall except for the case of $b/e = 1.17$ in which the Nusselt number is significantly lower than the results of flat plate. This is attributed to the rebound of wall jet, as discussed previously in the flow visualization experiments, which prevents its cooling effect. However, for $z/b = 8$ and 12, the average Nusselt numbers are very close to the results of the flat plate. This suggests that the rebound of wall jet does not occur when the wall jet becomes wide and turbulent before arriving at the wall. However, the rebound of wall jet was not found in the rectangular ribbed wall for case B.

3.2.2. Stagnation point Nusselt number

Comparison of the stagnation point Nusselt number between the case of the ribbed wall and the case of the flat plate is shown in Fig. 9. In general, the stagnation point Nusselt number on both the ribbed wall and the flat plate increases with the slot width. However, the rate of increase is different. When formation of an air bubble enclosing the cavity on the ribbed wall occurs, the stagnation point Nusselt number is significantly lower than in the case of the flat plate. This is the case for $z/b \leq 6$ when the impinging jet before arriving at

the wall is still laminar. For $z/b \geq 8$, that is the case when the impinging jet before arriving at the wall is relatively wide and turbulent which can readily penetrate the air bubble enclosing the cavity and significantly enhance heat transfer. Thus, the Nusselt number on the ribbed wall for these cases are significantly higher than for the flat plate. However, this is not true for a smaller slot width, i.e. $b/e = 1.17$. The Nusselt number on the ribbed wall for $b/e = 1.17$ is significantly lower than in the case on the flat plate even when $z/b \geq 8$. This is apparently due to the formation of air bubbles which prevent wall jet from penetrating into the cavity and reduce the heat transfer. Similar reduction of the heat transfer due to formation of air bubble enclosing the cavity was also found in rectangular ribbed wall. However, the formation of air bubble enclosing the cavity in the rectangular ribbed wall can be more readily initiated which occurs for both $b/e = 1.17$ and 2 when $z/b \geq 8$. The maximum Nusselt number at the stagnation point for the triangular ribbed wall occurs at $z/b = 10$ while for the flat plate it occurs at $z/b = 8$. This is apparently due to the effect of rib protrusion and formation of air bubble enclosing the cavity.

Comparison of the stagnation point Nusselt number for $p/e = 2$ and $p/e = 4$ is shown in Fig. 10. The stagnation point Nusselt number on the ribbed wall for both $p/e = 2$ and 4 increases with increasing b/e. However, the stagnation point Nusselt number for $p/e = 4$ is, in general, higher than for $p/e = 2$, except for the case of $p/e = 2$, $b/e \geq 4$ and $z/b \geq 8$. This is due to the fact that the air bubble enclosing the cavity around the stagnation point for $p/e = 4$ is relatively large as compared with the case of $p/e = 2$, and the wall jet can more readily penetrate the air bubble and impinge on the wall. This leads to a higher Nusselt number at and around the stagnation point for $p/e = 4$. However, the former discussion is not true when the slot width becomes wider and the impinging jet becomes turbulent before arriving at the wall. This is the case when the turbulent impinging jet can penetrate the air bubble enclosing the cavity and recirculate inside. One can expect that a smaller cavity (in the case of $p/e = 2$) will have higher circulation intensity than a larger cavity (in the case of $p/e = 4$). Therefore, the higher stagnation point Nusselt number for $p/e = 2$ than for $p/e = 4$, when $b/e \geq 4$ and $z/b \geq 8$, is attributed to a higher circulation intensity of the impinging jet in the cavity. The maximum Nusselt number at the stagnation point for both $p/e = 2$ and 4 occurs at $z/b = 10$ except for the case of $p/e = 2$ and $b/e \leq 2$ where the maximum occurs at z/b greater than 10. The exception is attributed to the occurrence of air bubble enclosing the cavity around the stagnation point which prevents the wall jet cooling effect even when the impinging jet becomes turbulent before arriving at the wall. However, once the turbulent jet penetrates the air bubble and recirculates inside at certain values of z/b, it can significantly enhance the heat transfer.

The stagnation point Nusselt numbers for the case when the impinging jet is directed towards the rib and the case when it is directed toward the center line of the cavity are compared in Fig. 11. In general, the stagnation point Nusselt number for case A is higher than for case B. This is due to the fact that the impinging jet for case A can more readily penetrate the air

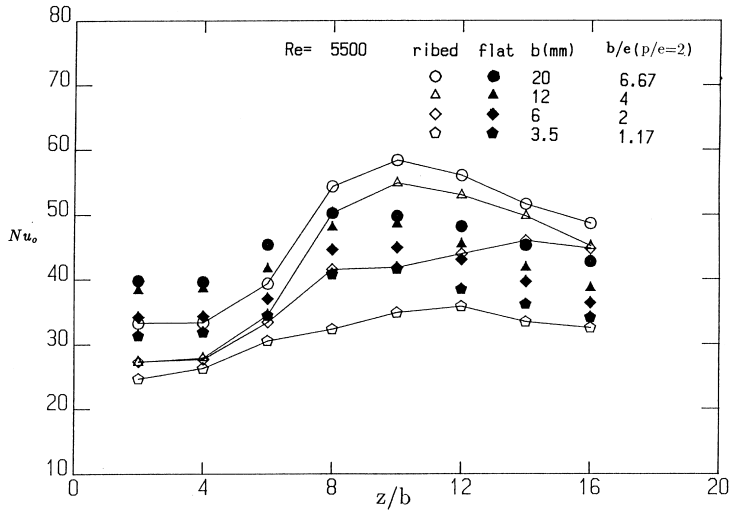

Fig. 9. Comparison of the stagnation point Nusselt number between the case of flat plate and the case of ribbed wall for Re = 5500.

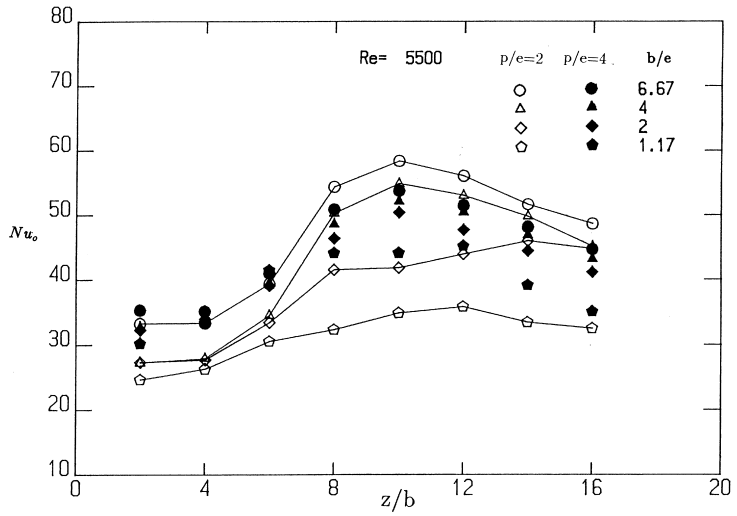

Fig. 10. Comparison of the stagnation point Nusselt number between the case of $p/e = 2$ and the case of $p/e = 4$ for $Re = 5500$.

bubble enclosing the cavity and impinge on the wall. In addition, the protrusion of the ribs increases the local surface area at the location where the rib stands, which can increase the total heat transfer rate and the heat transfer coefficient that is calculated based on the base area of the rib. The maximum Nusselt number at the stagnation point for both case A and case B occurs at $z/b = 10$, which is completely different from the results of the flat plate. For rectangular ribbed wall, the maximum occurs at $z/b = 8$ which is different from the case of the triangular ribbed wall. It appears that in addition to the formation of air bubble and the total surface area of the rib, the geometric shape of the ribs has also some effect on the stagnation point heat transfer. This is also true at higher Reynolds numbers.

3.2.3. Correlation of stagnation point Nusselt number

The stagnation point Nusselt number increases monotonically with increasing slot width-to-rib height ratio at both low and high Reynolds numbers. Correlations of Nu_o in terms of the Reynolds number, the slot width-to-rib height ratio, the nozzle-to-plate spacing and the rib pitch-to-height ratio can be made. However, better correlations can be obtained as follows if the correlations for $z/b \leq 10$ and $z/b \geq 10$ are made separately:

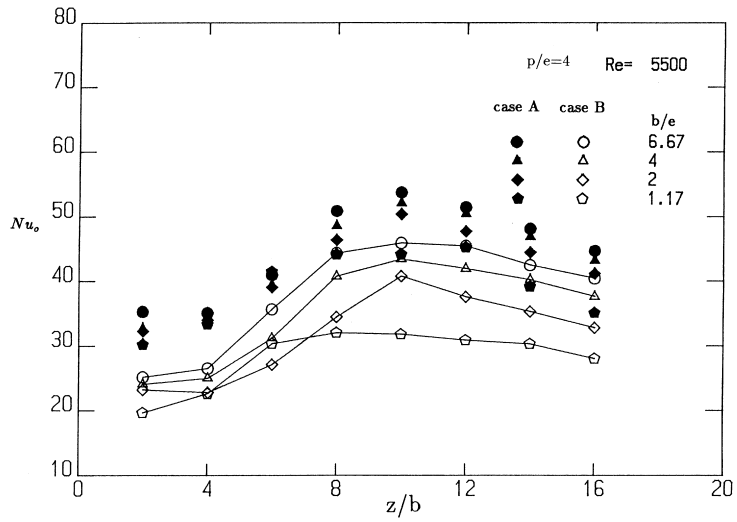

Fig. 11. Comparison of the stagnation point Nusselt number between case A and case B for $p/e = 4$ and $Re = 5500$.

For case A with $2 \le z/b \le 10$, the least square fit of data is

$$Nu_o = 0.097(b/e)^{0.125}(p/e)^{0.24}(Re)^{0.58}(z/b)^{0.3} \quad (2)$$

where the standard deviation of the data is 3.686. For case A with $10 \le z/b \le 16$,

$$Nu_o = 0.535(b/e)^{0.19}(p/e)^{0.0037}(Re)^{0.56}(z/b)^{-0.25} \quad (3)$$

where the standard deviation of the data is 3.6. For case B with $2 \le z/b \le 10$,

$$Nu_o = 0.093(b/e)^{0.17}(p/e)^{-0.073}(Re)^{0.59}(z/b)^{0.37} \quad (4)$$

where the standard deviation of the data is 3.29. For case B with $10 \le z/b \le 16$,

$$Nu_o = 0.7(b/e)^{0.22}(p/e)^{-0.19}(Re)^{0.53}(z/b)^{-0.24} \quad (5)$$

where the standard deviation of the data is 2.93.

The above correlations are valid for $2750 \le Re \le 11{,}000$, $1.17 \le b/e \le 6.67$ and $2 \le p/e \le 4$. It appears that the stagnation point Nusselt number increases with increasing z/b for $z/b \le 10$, but decreases

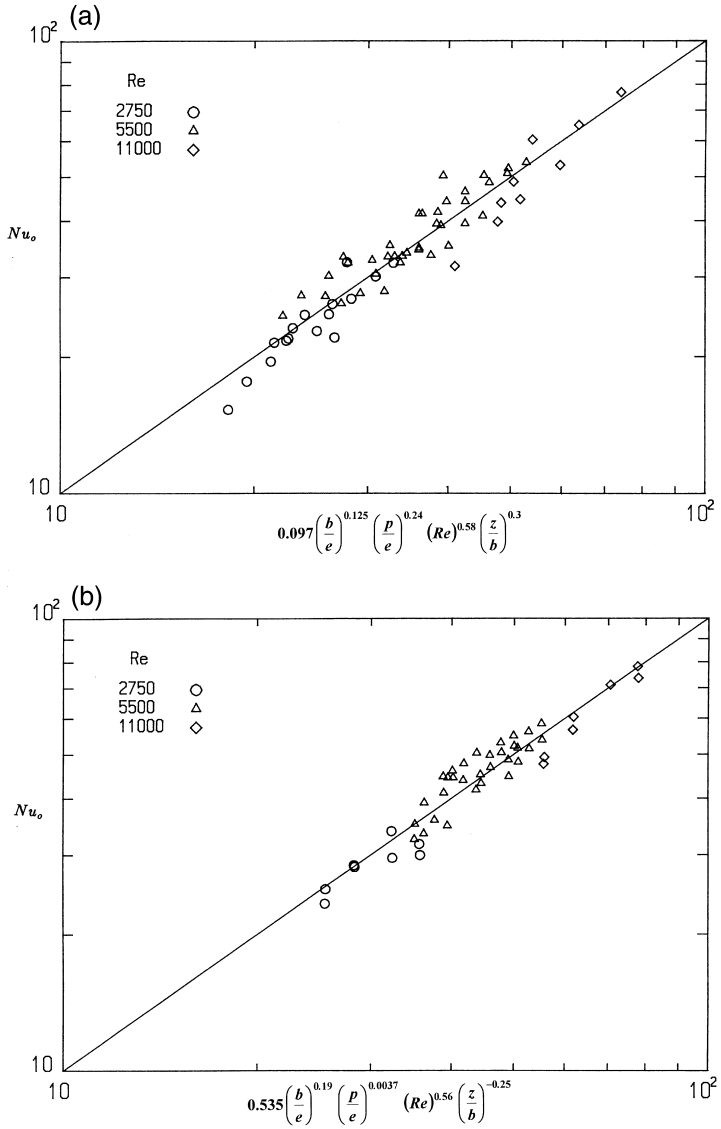

Fig. 12. Correlations of the stagnation point Nusselt number for case A with $2750 \le Re \le 11{,}000$, $1.17 \le b/e \le 6.67$, $2 \le p/e \le 4$, and (a) $2 \le z/b \le 10$, (b) $10 \le z/b \le 16$.

with increasing z/b for $z/b \geq 10$. However, the effect of p/e on the Nu_o for case A is different from case B. For case A, Nu_o increases with increasing p/e while for case B, Nu_o decreases with increasing p/e. It appears that for case A and $z/b \leq 10$ the air bubble formed on the ribbed wall at larger p/e is greater which can let the wall jet more readily penetrate inside and impinge on the wall to enhance the heat transfer. However, when the impinging jet before arriving at the wall becomes turbulent, it can readily penetrate into the air bubble for both $p/e = 2$ and 4. For case B with $z/b \leq 10$, the pressure of the air bubble on the stagnation point is so large that penetration of the wall jet into the cavity become difficult for both $p/e = 2$ and 4. This leads to the result that the size of the rib pitch has almost no effect on Nu_o. However, formation of air bubble still occurs for case B when the impinging jet before arriving at the wall becomes turbulent. However, penetration of the wall jet into air bubble and recirculation inside occur. It appears that circulation in the smaller cavity is more intense than in larger cavity and leads to a higher Nu_o for a smaller p/e. This peculiar phenomenon was not found in rectangular ribbed walls. Typical least square fit of the data is presented in Fig. 12a and b.

4. Conclusions

Impingement cooling flow structure and wall heat transfer along triangular ribbed walls has been studied. Both flow visualization and local Nusselt number measurements along the ribbed wall are made. Formation of air bubbles enclosing cavities in the region around the stagnation point were found in triangular ribbed wall, which can reduce the heat transfer and make it even lower than in the case of the flat plate. However, as the impinging or the wall jet becomes turbulent, it can readily penetrate the air bubble, impinge on the wall and significantly enhance the heat transfer. However, the cavity is wide open which makes the impinging or the wall jet more readily penetrate into the cavity and impinge on the wall than in the case along the rectangular ribbed wall. The strong momentum exchange between the cavity flow and the wall jet makes the recirculation cell scarce in the cavity. In this way, the heat transfer along the triangular ribbed wall is better. However, the smaller surface area of the triangular rib has limited the enhancement. In addition, the geometric shape of the triangular rib is favourable for rebounding the wall jet away from the wall. This can significantly reduce heat transfer and make it lower than in the case of the flat plate.

The results of the stagnation point heat transfer are also presented and correlated. Nu_o for case A is found to increase with increasing p/e while Nu_o for case B is found to decrease. This peculiar phenomenon was not found on rectangular ribbed wall. The higher Nu_o at smaller p/e is attributed to the more intense circulation flow in the smaller cavity of the triangular ribbed wall.

Acknowledgements

This research was sponsored by the National Science Council of Taiwan under contract No. NSC 82-0401-E006-433.

References

[1] Y. Becko, Impingement Cooling — a Review, Von Karman Institute for Fluid Dynamics, Lecture Series 83, 1976.
[2] H. Martin, Heat and mass transfer between impinging gas jets and solid surfaces, in: J. Hartnett, T. Irvine Jr (Eds.), Advance in Heat Transfer, vol. 13, 1977, pp. 1–60.
[3] J.W. Baughn, S. Shimizu, Heat transfer measurements from a surface with uniform heat flux and an impinging jet, Journal of Heat Transfer 111 (1989) 1097–1100.
[4] R. Gardon, J.C. Akeirat, Heat transfer characteristics of impinging two-dimensional air jet, Journal of Heat Transfer 88 (1966) 101–108.
[5] R.J. Goldstein, J.F. Timmers, Visualization of heat transfer from arrays of impinging jets, International Journal of Heat and Mass Transfer 25 (1982) 1857–1868.
[6] P. Hrycak, Heat transfer from round impinging jets to a flat plate, International Journal of Heat and Mass Transfer 26 (1983) 1857–1865.
[7] M. Korger, F. Krizek, Mass-transfer coefficient in impingement flow from slotted nozzles, International Journal of Heat and Mass Transfer 9 (1981) 337–344.
[8] R.J. Goldstein, M.E. Franchett, Heat transfer from a flat surface to an oblique impinging jet, Journal of Heat Transfer 110 (1988) 84–90.
[9] C.D. Donaldson, R.S. Snedeker, A study of free jet impingement. Part 1: mean properties of free impinging jets, Journal of Fluid Mechanics 45 (1971) 281–319.
[10] C.D. Donaldson, R.S. Snedeker, A study of free jet impingement. Part 2: free jet turbulent structure and impingement heat transfer, Journal of Fluid Mechanics 45 (1971) 477–512.
[11] P. Hrycak, Heat transfer from a row of impinging jets to concave cylindrical surfaces, International Journal of Heat and Mass Transfer 24 (1980) 407–419.
[12] C. Gau, C.M. Chung, Surface curvature effect on slot-air-jet impingement cooling flow and heat transfer process, Journal of Heat Transfer 113 (1991) 858–864.
[13] R.L. Webb, in: Principles of Enhanced Heat Transfer, Wiley, New York, 1994, pp. 229–284 (Chapter 9).
[14] C. Gau, C.C. Lee, Impingement cooling flow structure

and heat transfer along rib-roughened walls, International Journal of Heat Mass Transfer 35 (1992) 3009–3020.

[15] I.C. Lee, Impingement cooling flow and heat transfer along triangular rib-roughened walls, M.S. Thesis, National Cheng Kung University, Tainan, Taiwan, 1994.

[16] S.J. Kline, F.A. McClintock, Describing uncertainties in single-sample experiments, Mechanical Engineering 73 (1953) 3–8.